

High-Temperature Thermal Decomposition of Benzyl Radicals[†]

Matthew A. Oehlschlaeger,[‡] David F. Davidson,* and Ronald K. Hanson

High-Temperature Gasdynamics Laboratory, Department of Mechanical Engineering, Stanford University, Stanford, California, 94305-3032

Received: September 22, 2005; In Final Form: November 1, 2005

The thermal decomposition of the benzyl radical was studied in shock tube experiments using ultraviolet laser absorption at 266 nm for detection of benzyl. Test gas mixtures of 50 and 100 ppm of benzyl iodide dilute in argon were heated in reflected shock waves to temperatures ranging from 1430 to 1730 K at total pressures around 1.5 bar. The temporal behavior of the 266 nm absorption allowed for determination of the benzyl absorption cross-section at 266 nm and the rate coefficient for benzyl decomposition, $C_6H_5CH_2 \rightarrow C_7H_6 + H$. The rate coefficient for benzyl decomposition at 1.5 bar can be described using a two-parameter Arrhenius expression by $k_1(T) = 8.20 \times 10^{14} \exp(-40\,600\text{ K}/T) [s^{-1}]$, and the benzyl absorption cross-section at 266 nm was determined to be $\sigma_{\text{benzyl}} = 1.9 \times 10^{-17} \text{ cm}^2 \text{ molecule}^{-1}$ with no discernible temperature dependence over the temperature range of the experiments.

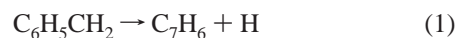
Introduction

The benzyl radical ($C_6H_5CH_2$) plays an important role in the oxidation and pyrolysis of toluene and other aromatics. Benzyl is generated as an intermediate at significant concentrations during the oxidation of toluene via the reaction of toluene with molecular oxygen, the reaction of toluene with radical species, and the toluene thermal decomposition channel leading to benzyl radicals and H-atoms. Because benzyl radicals are a primary intermediate on the toluene oxidation pathway, the rates of reactions which consume benzyl radicals, such as benzyl decomposition, are of crucial importance in modeling the oxidation of toluene and other aromatic fuels. Additionally, the decomposition of benzyl is important in modeling soot formation, because it competes with the formation of naphthalene which occurs via reaction of benzyl with propargyl.

The decomposition of benzyl radicals has been previously studied using several different experimental techniques. Smith first investigated the thermal decomposition of toluene in a Knudsen cell with mass spectrometry recommending benzyl decomposition channels leading to either $C_3H_3 + C_4H_4$ or $C_2H_2 + C_5H_5$ fragments.¹ Troe, Hippler, and co-workers^{2–6} have investigated the decomposition of benzyl radicals in shock tube experiments using time-resolved ultraviolet absorption for detection of benzyl with toluene, benzyl iodide, benzyl chloride, and methyl benzyl ketene as benzyl precursors. Their series of investigations led to the conclusion that one H-atom is produced per dissociated benzyl radical.⁶ Shock tube experiments using time-resolved H-atom ARAS to investigate the decomposition of benzyl have been performed by Braun-Unkoff et al.⁷ and Rao and Skinner.⁸ Both studies concluded that benzyl decomposition yielded a C_7H_6 fragment of unknown structure and an H-atom. Using a single-pulse shock tube with analysis of the product gas via flame ionization detection, Colket and Seery⁹

recommended product channels that lead to both $C_3H_3 + C_4H_4$ and $C_2H_2 + C_5H_5$ fragments as originally proposed by Smith.¹ Most recently, Jones et al.¹⁰ shock-heated benzyl bromide, investigating benzyl decomposition using ultraviolet absorption, and performed quantum chemical calculations to recommend product channels; their calculations indicated that product channels leading to either $C_5H_5 + C_2H_2$ or $C_7H_6 + H$ were possible.

In addition to the shock tube experiments, Fröchtenicht et al.¹¹ have performed experiments using photon-induced decomposition of benzyl radicals in a molecular beam with mass spectrometry detection. Their mass spectrometry results conclusively determined that the product species for benzyl photolysis are a C_7H_6 fragment and an H-atom. The agreement between the Fröchtenicht et al. experiment and the shock tube experiments using time-resolved ultraviolet absorption (Hippler et al.⁶) and H-atom ARAS (Braun-Unkoff et al.⁷) support the conclusion that the benzyl radical decomposes to yield an H-atom and a C_7H_6 fragment of unknown structure (reaction 1)



In addition, recently, Eng et al.¹² investigated toluene decomposition using H-atom ARAS and found that the growth of H-atoms during toluene decomposition could not be modeled without accounting for the decomposition of benzyl radicals to yield one H-atom per benzyl. The observation of C_5H_5 , C_4H_4 , C_3H_3 , and C_2H_2 products in the Knudsen cell experiments of Smith¹ and the single-pulse shock tube experiments of Colket and Seery⁹ are most likely the result of further fragmentation reactions, rather than direct decomposition of benzyl. The chemical structure of the C_7H_6 product has yet to be identified, although Braun-Unkoff et al.⁷ and Jones et al.¹⁰ both suggest a chain ring-opening pathway with a C_7H_6 product of aliphatic structure $H_2C=C=CH-HC=CH-C\equiv CH$.

Despite the agreement for the H-atom product stoichiometry for benzyl decomposition, previous experimental studies show disagreement among each other for the benzyl decomposition rate coefficient. In this work, we present measurements of

[†] Part of the special issue "David M. Golden Festschrift".

* Corresponding author. David Davidson, Stanford University, Bldg 520, Room 520I, Stanford, CA, 94305-3032. Phone: 650-725-2072. Fax: 650-723-1748. dfd@stanford.edu.

[‡] Current affiliation: Department of Mechanical, Aerospace, and Nuclear Engineering, Rensselaer Polytechnic Institute, Troy, New York.

reaction 1 using laser absorption at 266 nm due primarily to benzyl radicals. The experiments were performed by shock-heating mixtures of 50 or 100 ppm of benzyl iodide diluted in argon to temperatures of 1430–1730 K around a pressure of 1.5 bar. The mixtures chosen were dilute enough to maintain isolated sensitivity to the rate coefficient of interest, k_1 , and the temperature range was chosen to ensure immediate decomposition of the benzyl iodide following the reflected shock wave and to avoid interference from benzyl association to form dibenzyl. The use of laser absorption in the current experiments provided a substantial increase in signal-to-noise in comparison to the previous ultraviolet absorption measurements made in this reaction system, which were carried out using less spectrally bright ultraviolet lamp sources. Therefore, the current measurements provide rate coefficient results with reduced uncertainty. In addition to the benzyl decomposition rate coefficient determination, the 266 nm absorption profiles allow for the determination of the benzyl absorption cross-section at 266 nm.

Experimental Section

Shock Tube Apparatus and 266 nm Laser Source. The experiments reported here were performed behind reflected shock waves in a pressure-driven stainless steel shock tube. The driven section is 8.54 m long, and the driver is 3.35 m long; both sections are 14.13 cm in inner diameter. Prior to each experiment, the driven section was evacuated with a vacuum system consisting of a zeolite-trapped mechanical pump and a Varian V-250 turbomolecular pump, providing ultimate pressures of 10^{-7} Torr with a typical leak rate of 10^{-6} Torr per minute. Shock velocities were measured with five piezoelectric pressure transducers spaced axially over the last 1.5 m of the tube. The signals from the five transducers were sent to four Philips PM6666 counter timers with resolution of 0.1 μ s to determine the shock passage time interval. The shock velocities measured from the shock passage time intervals were extrapolated to the endwall using a linear attenuation profile with typical velocity attenuation rates of 0.8–1.5% per meter. In addition to the five pressure transducers used for shock velocity, an additional Kistler transducer (603B1 transducer and 5010B amplifier) was used to measure the pressure time history during shock-heating. The preshock initial mixture pressure was measured using high-accuracy Baratron capacitance manometers. The incident and reflected shock conditions were calculated using the normal shock equations and the measured incident shock velocity; uncertainty in the experimental pressure and temperature are $\sim 1\%$ and $\sim 0.7\%$, respectively, with the primary contribution being uncertainty in the measured shock velocity.

Mixtures were made in a turbo-pumped stainless steel mixing tank (12 L) with an internal stirring system. Research-grade argon (99.999%) was used as the driven carrier gas. Benzyl iodide, supplied by the Narchem Corporation (Chicago, IL) at 99% purity, was mixed with argon in the mixing tank at concentrations of 50 and 100 ppm prior to experiments. Benzyl iodide has a fusion temperature of 24.5 $^{\circ}$ C at 1 bar. Therefore, for the successful introduction of benzyl iodide into the mixing tank, the room temperature was raised to 26 $^{\circ}$ C to increase the benzyl iodide vapor pressure, and the tank was heated to 35 $^{\circ}$ C and 45 $^{\circ}$ C using a resistance heating tape to avoid wall condensation and adsorption. The two sets of experiments (mixing tank at 35 $^{\circ}$ C and 45 $^{\circ}$ C) resulted in identical 266 nm benzyl absorption cross-section results providing confidence that the benzyl iodide concentration in the mixtures was accurate, as determined manometrically, and wall adsorption was not affecting the mixtures. Additionally, the benzyl iodide was

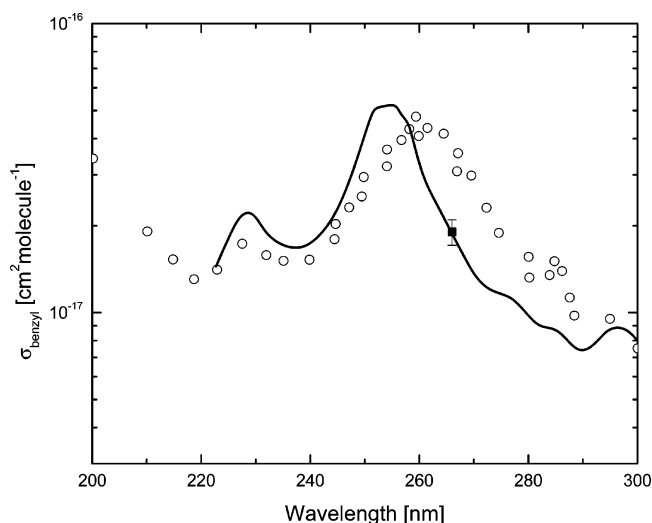


Figure 1. Hot benzyl radical spectrum: open circles, Müller-Markgraf and Troe⁵ (1600 K, shock tube); solid line, Ikeda et al.¹³ (estimated at 1300 K, laser flash photolysis); solid square, this study (1430–1730 K).

cycled through several freeze–pump–thaw cycles prior to introduction into the mixing tank to avoid impurities from high-volatility species. Mixtures were allowed to mix overnight prior to shock wave experiments to allow for complete mixing.

Benzyl radicals have strong broadband absorption in the ultraviolet from 245 to 275 nm^{5,13} (see Figure 1) allowing detection of benzyl at 266 nm. Continuous-wave laser radiation was generated at 266 nm (1.5 mW) by the single pass of a focused 532 nm laser beam (Nd:YVO₄ at 5 W) through an angle-tuned β -barium borate (β -BaB₂O₄, BBO) crystal. After generation, the harmonic (266 nm) was separated from the fundamental (532 nm) in a Pellin-Broca prism. The 266 nm laser beam was split into two components: one, ~ 1 mm in diameter, passing through the shock tube as a diagnostic beam (I), and one detected prior to absorption as a reference (I_0). Optical measurements were made at a location 2 cm from the endwall. The shock-heated gases were accessed through 0.75-in-diameter flat wedged windows made of UV fused silica flush-mounted to the inner radius of the shock tube. The intensity of the reference and diagnostic beams was measured using amplified silicon photodiodes (Hamamatsu S1722-02, rise time $< 0.5 \mu$ s, 4.1 mm diameter) and recorded on a digital oscilloscope. The measured fractional absorption (I/I_0) is related to absorption cross-section and the benzyl concentration via Beer's law

$$I/I_0 = \exp(-\text{absorbance}) = \exp(-\sigma_{\text{benzyl}} n_{\text{benzyl}} L)$$

where I is the transmitted laser intensity, I_0 is the reference beam intensity, σ_{benzyl} [$\text{cm}^2 \text{ molecule}^{-1}$] is the benzyl absorption cross-section, n_{benzyl} [molecules cm^{-3}] is the benzyl number density, and L is the absorption path length (diameter of the shock tube 14.13 cm).

Determination of Benzyl 266 nm Absorption Cross-Section and Decomposition Rate Coefficient. Benzyl radicals ($\text{C}_6\text{H}_5\text{-CH}_2$) were generated immediately behind reflected shock waves by the dissociation of benzyl iodide



allowing the determination of both the absorption cross-section of benzyl at 266 nm and the rate coefficient for benzyl decomposition, k_1 . The absorbance at 266 nm for an example experiment is shown in Figure 2. Prior to the incident shock

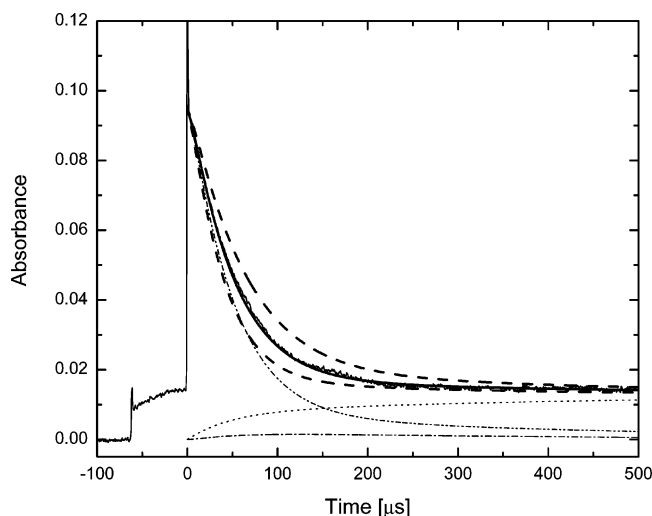
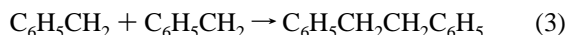


Figure 2. Example 266 nm absorbance during benzyl iodide decomposition. Reflected shock conditions: 1615 K, 1.54 bar, 50 ppm benzyl iodide/Ar. Solid line, best fit to absorbance by adjusting k_1 ; dashed lines, variation of $k_1 \pm 25\%$; dot-dot-dashed line, contribution to absorbance from benzyl; dotted line, contribution to absorbance from benzyl fragments; dot-dashed line, contribution to absorbance from toluene.

wave, no absorption by benzyl iodide was detected at the low initial pressure, P_1 . The passing of the incident shock wave causes a schlieren spike in the signal, and the test gas is compressed and heated, causing the benzyl iodide to absorb (1% absorbance at $t \approx -60 \mu\text{s}$ in Figure 2). Behind the incident shock wave, the benzyl iodide ($\text{C}_6\text{H}_5\text{CH}_2\text{-I}$ bond strength 51 kcal/mol) slowly dissociates into the more strongly absorbing benzyl radical and an I-atom. While the incident shock temperature is not sufficient to induce benzyl radical decomposition, the benzyl can combine to give stable dibenzyl

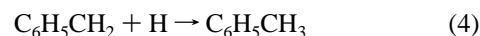


The passage of the reflected shock wave causes another schlieren spike in the absorbance trace and immediately ($< 1 \mu\text{s}$) causes complete dissociation of the benzyl iodide and the small amount of dibenzyl (benzyl-benzyl bond strength 65.2 kcal/mol) that was formed in the incident test time. Thus, the test gas mixture yields one benzyl radical per benzyl iodide precursor at $t = 0$, allowing determination of the 266 nm absorption cross-section for benzyl. The absorbance at $t = 0$ was determined by back-

extrapolating the steady decay in the absorbance signal to $t = 0$, defined as the center of the schlieren spike. The results for the 266 nm benzyl absorption cross-section are given in Figure 4. The measured benzyl absorption cross-section showed no discernible temperature dependence from 1430 to 1730 K and was found to be $\sigma_{\text{benzyl}}(266 \text{ nm}) = 1.9 (\pm 0.2) \times 10^{-17} \text{ cm}^2 \text{ molecule}^{-1}$. Uncertainty in the measured cross-section is primarily due to uncertainty in the initial benzyl iodide concentration in the test gas mixtures.

After the peak in absorption following the reflected shock, the 266 nm absorption decays because of benzyl decomposition, reaction 1, forming more weakly absorbing benzyl fragments. Before examining the decay in the 266 nm absorption to extract k_1 , the interfering absorption due to the benzyl fragments was quantified. The absorbance at long times (Figure 2) decays to approximately a constant value. Under the assumption of a complete one-to-one conversion of benzyl to benzyl fragments at long times, the 266 nm absorption cross-section of the benzyl fragments was determined from the value of the absorbance at long times; see Figure 5 for the results for the benzyl fragment absorption cross-section. As in the case of benzyl, the benzyl fragment 266 nm cross-section showed no temperature dependence in the range of these experiments and was determined to be $\sigma_{\text{fragment}}(266 \text{ nm}) = 3.4 (\pm 0.5) \times 10^{-18} \text{ cm}^2 \text{ molecule}^{-1}$.

To determine the rate coefficient for benzyl decomposition, the decay in absorbance was fit by adjusting k_1 within a reaction mechanism, given in Table 1, and by accounting for the contributions to the absorption due to benzyl, benzyl fragments, and toluene. Toluene is formed at small concentrations in these experiments by the secondary reaction



The toluene 266 nm absorption cross-section was determined in separate toluene shock tube experiments to be $\sigma_{\text{toluene}}(266 \text{ nm}) = 5.9 (\pm 0.6) \times 10^{-19} \text{ cm}^2 \text{ molecule}^{-1}$.²⁴

The reaction mechanism used to model the measurements described here was developed primarily by Troe, Hippler, and co-workers.^{5,6,14,15,19,20} Fortunately, the low concentrations of benzyl iodide used in the test mixtures provide measurements which show little sensitivity to secondary chemistry. Therefore, excellent agreement between fit and experiment was obtained by adjusting only the rate coefficient for reaction 1. After the immediate decomposition of the benzyl iodide precursor, the benzyl is primarily consumed via reaction 1. However, the reaction of benzyl with H-atoms to form toluene, reaction 4,

TABLE 1: Reaction Mechanism Used for Modeling Benzyl Decomposition^a

| | reaction | A [cm, mol, s] | b | E_a [cal/mol] | ref |
|------|--|-----------------------|---|--------------------|------------|
| (1) | $\text{C}_6\text{H}_5\text{CH}_2 \rightarrow \text{C}_7\text{H}_6 + \text{H}$ (1.5 bar) | 8.20×10^{14} | 0 | 80670 | this study |
| (4) | $\text{C}_6\text{H}_5\text{CH}_2 + \text{H} \rightarrow \text{C}_6\text{H}_5\text{CH}_3$ | 2.00×10^{14} | 0 | 0 | (16) |
| | $\text{C}_6\text{H}_5\text{CH}_3 \rightarrow \text{C}_6\text{H}_5\text{CH}_2 + \text{H}$ (1.5 bar) | 2.09×10^{15} | 0 | 87507 | (24) |
| | $\text{C}_6\text{H}_5\text{CH}_3 \rightarrow \text{C}_6\text{H}_5 + \text{CH}_3$ (1.5 bar) | 2.66×10^{16} | 0 | 97880 | (24) |
| (2) | $\text{C}_6\text{H}_5\text{CH}_2\text{I} \rightarrow \text{C}_6\text{H}_5\text{CH}_2 + \text{I}$ | 5.89×10^{14} | 0 | 43260 | (5) |
| (-2) | $\text{C}_6\text{H}_5\text{CH}_2 + \text{I} \rightarrow \text{C}_6\text{H}_5\text{CH}_2\text{I}$ | 5.01×10^{13} | 0 | 0 | (5) |
| | $\text{C}_6\text{H}_5\text{CH}_3 + \text{H} \rightarrow \text{C}_6\text{H}_5\text{CH}_2 + \text{H}_2$ | 1.26×10^{15} | 0 | 14818 | (6) |
| | $\text{C}_6\text{H}_5 + \text{H} \rightarrow \text{C}_6\text{H}_6$ | 7.80×10^{13} | 0 | 0 | (17) |
| | $\text{H} + \text{C}_6\text{H}_5\text{CH}_3 \rightarrow \text{CH}_3 + \text{C}_6\text{H}_6$ | 5.78×10^{13} | 0 | 8090 | (16) |
| | $\text{CH}_3 + \text{C}_6\text{H}_5\text{CH}_3 \rightarrow \text{C}_6\text{H}_5\text{CH}_2 + \text{CH}_4$ | 3.16×10^{12} | 0 | 0 | (18) |
| | $\text{C}_6\text{H}_5 + \text{C}_6\text{H}_5\text{CH}_3 \rightarrow \text{C}_6\text{H}_6 + \text{C}_6\text{H}_5\text{CH}_2$ | 7.94×10^{13} | 0 | 11940 | (19) |
| (3) | $\text{C}_6\text{H}_5\text{CH}_2 + \text{C}_6\text{H}_5\text{CH}_2 \rightarrow \text{C}_6\text{H}_5\text{CH}_2\text{CH}_2\text{C}_6\text{H}_5$ | 5.01×10^{12} | 0 | 454 | (14) |
| | $\text{C}_6\text{H}_5\text{CH}_2\text{CH}_2\text{C}_6\text{H}_5 \rightarrow \text{C}_6\text{H}_5\text{CH}_2 + \text{C}_6\text{H}_5\text{CH}_2$ | 7.94×10^{14} | 0 | 59751 | (14) |
| | $\text{C}_6\text{H}_5\text{CH}_2\text{CH}_2\text{C}_6\text{H}_5 \rightarrow \text{C}_6\text{H}_5\text{CH}_2\text{CHC}_6\text{H}_5 + \text{H}$ | 1.00×10^{16} | 0 | 83660 | (20) |
| | $\text{C}_6\text{H}_5\text{CH}_2\text{CH}_2\text{C}_6\text{H}_5 + \text{H} \rightarrow \text{C}_6\text{H}_5\text{CH}_2\text{CHC}_6\text{H}_5 + \text{H}_2$ | 3.16×10^{12} | 0 | 0 | (15) |
| | $\text{C}_6\text{H}_5\text{CH}_2\text{CHC}_6\text{H}_5 \rightarrow \text{C}_6\text{H}_5\text{CHCHC}_6\text{H}_5 + \text{H}$ | 7.94×10^{15} | 0 | 51864 | (15) |

^a Rate coefficients in the form $k = AT^b \exp(-E_a/RT)$.

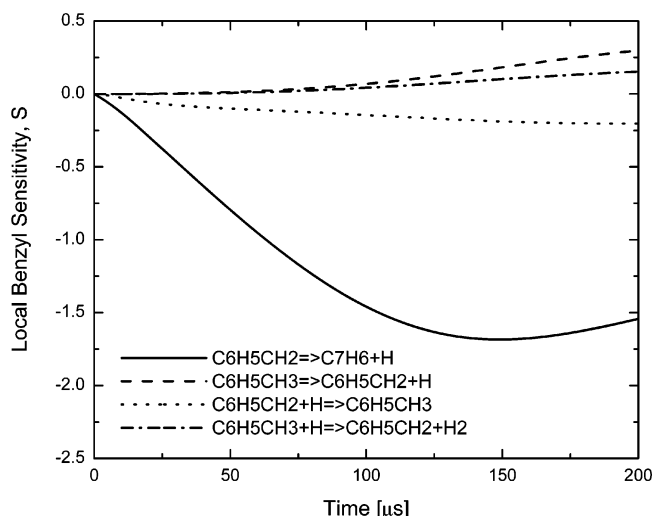


Figure 3. Local sensitivity for benzyl concentration for conditions of experiment given in Figure 2. $S = (dX_{\text{benzyl}}/dk_i)(k_i/X_{\text{benzyl,local}})$, where k_i is the rate constant for reaction i and $X_{\text{benzyl,local}}$ is the local benzyl ($\text{C}_6\text{H}_5\text{-CH}_2$) mole fraction.

TABLE 2: Summary of Experimental Results

| mixture | temperature [K] | pressure [bar] | k_1 [1/s] |
|--------------------------|-----------------|----------------|-------------------|
| 100 ppm benzyl iodide/Ar | 1461 | 1.64 | 6.5×10^2 |
| | 1499 | 1.57 | 1.6×10^3 |
| | 1551 | 1.56 | 4.1×10^3 |
| | 1601 | 1.51 | 9.0×10^3 |
| | 1669 | 1.45 | 2.3×10^4 |
| | 1669 | 1.44 | 2.5×10^4 |
| | 1680 | 1.44 | 2.7×10^4 |
| | 1704 | 1.48 | 3.9×10^4 |
| 50 ppm benzyl iodide/Ar | 1715 | 1.46 | 3.9×10^4 |
| | 1428 | 1.63 | 3.0×10^2 |
| | 1522 | 1.58 | 2.5×10^3 |
| | 1566 | 1.47 | 5.0×10^3 |
| | 1610 | 1.52 | 9.2×10^3 |
| | 1615 | 1.54 | 9.8×10^3 |
| | 1700 | 1.45 | 2.9×10^4 |
| | 1730 | 1.47 | 5.1×10^4 |

and the association of benzyl to yield dibenzyl, reaction 3, were included in the mechanism. Secondary chemistry accounting for the decomposition of toluene and toluene + radical reactions was also included along with the dibenzyl reaction pathways to form stilbene proposed by Hippler et al.⁶ Kinetic computations were performed using CHEMKIN 2.0²¹ and SENKIN.²² The sensitivity for benzyl concentration for the experiment shown in Figure 2 is given in Figure 3. Notice that the benzyl concentration shows isolated sensitivity to reaction 1 over the first 100 μs , allowing a direct fit without interference from secondary reactions. The isolated sensitivity to reaction 1, due to the low concentration of benzyl iodide precursor, provides a nearly first-order fit only complicated by interfering absorption. Therefore, uncertainties in the initial concentration of benzyl iodide and the benzyl absorption cross-section do not affect the uncertainty in the rate coefficient determination.

The rate coefficient determinations for reaction 1 are tabulated in Table 2 and shown in Figure 6 on an Arrhenius plot along with a least-squares fit. The first-order rate coefficient at 1.5 bar given by the least-squares fit can be expressed as

$$k_1(T) = 8.20 \times 10^{14} \exp(-40\,600 \text{ K}/T) [\text{s}^{-1}]$$

where the root-mean-square (rms) experimental scatter about the fit is $\pm 11\%$. The overall uncertainty of the rate coefficient is

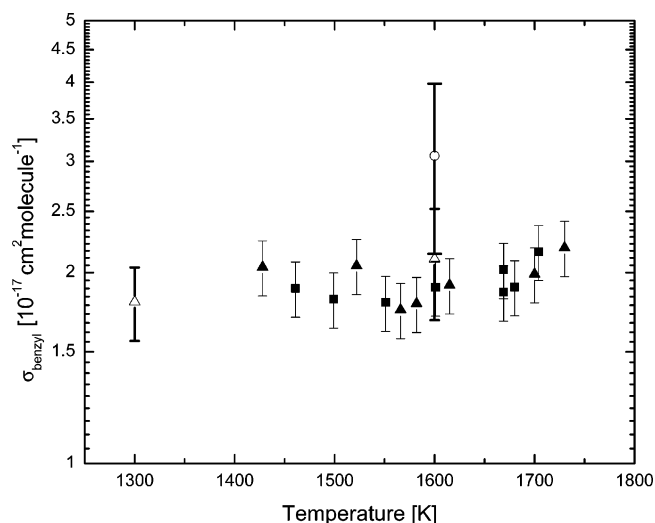


Figure 4. Benzyl radical absorption cross-section at 266 nm: solid squares, this study—100 ppm benzyl iodide/Ar; solid triangles, this study—50 ppm benzyl iodide/Ar; open triangle, Ikeda et al.;¹³ open circle, Müller-Markgraf and Troe.⁵

estimated at $\pm 25\%$. The primary contributions to the uncertainty in the rate coefficient are uncertainties in temperature, fitting the data to computed profiles, and interfering absorption.

Discussion

The results for the absorption cross-section of benzyl radicals and benzyl fragments are given in Figures 1, 4, and 5 with comparison to previous experimental studies. The results for the benzyl radical absorption cross-section are in good agreement with the flash photolysis measurement of Ikeda et al.¹³ but are about 50% lower than the shock tube results of Müller-Markgraf and Troe;⁵ see Figures 1 and 4. Müller-Markgraf and Troe examined the absorption spectra of benzyl behind shock waves at 1600 K using a Xe high-pressure discharge lamp dispersed with a monochromator. In comparison to the laser absorption measurements presented here, the Müller-Markgraf and Troe lamp measurements have absorbance noise at least a factor of 10 larger because of the limited spectral brightness and optical collection efficiency of their lamp absorption measurements. Therefore, the resulting absorption cross-section measured by Müller-Markgraf and Troe is significantly less certain than the current measurement (error bars in Figures 4 and 5 are estimated on the basis of scatter in the data of Müller-Markgraf and Troe⁵). However, the results of the current benzyl fragment absorption cross-section measurements are in excellent agreement with the measurements of Müller-Markgraf and Troe (Figure 5).

Comparison of the results presented here for k_1 with the results of four previous shock tube studies is shown in Figure 6. The current data agree very well with the UV absorption study of Hippler et al.⁶ (~ 0.5 bar) and the H-atom ARAS study of Braun-Unkoff et al.⁷ (~ 2 bar), although the scatter of the current data is significantly reduced from that of these previous studies. In addition, the current data for k_1 is in agreement with the International Union of Pure and Applied Chemistry (IUPAC) review recommendation (Baulch et al.²³). (The IUPAC review recommends the rate coefficient previously determined by Braun-Unkoff et al.⁷) The rate coefficient results of shock tube study of Jones et al.¹⁰ (~ 10 – 12 bar) complemented with quantum chemical calculations and the H-atom ARAS study of Rao and Skinner⁸ (~ 0.6 bar) are approximately an order of magnitude lower than the results of the current study. The experimental rate determinations of Jones et al.¹⁰ have scatter of approx-

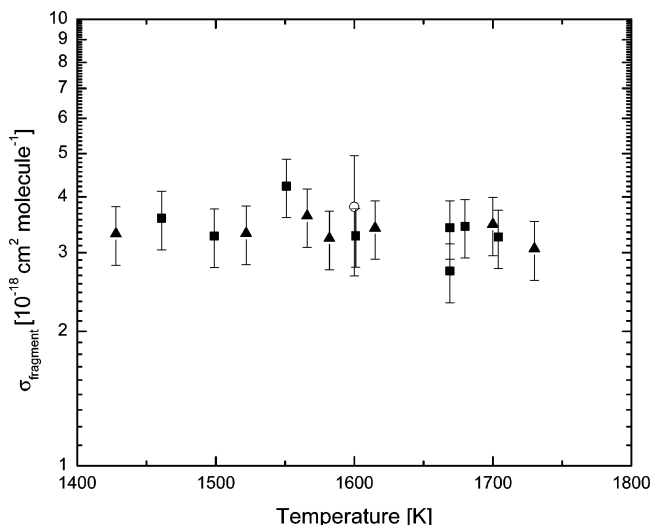


Figure 5. Benzyl fragment absorption cross-section at 266 nm: solid squares, this study—100 ppm benzyl/Ar; solid triangles, this study—50 ppm benzyl iodide/Ar; open circle, Müller-Markgraf and Troe.⁵

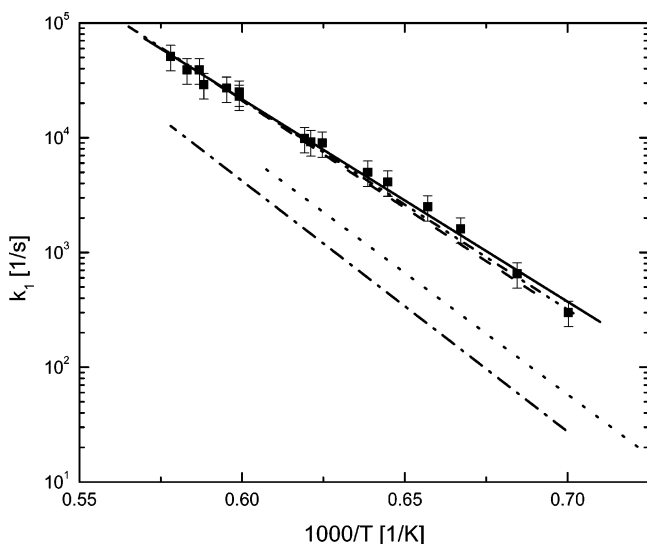


Figure 6. Rate coefficient for benzyl decomposition, reaction 1: filled squares with error bars, current experimental results (~1.5 bar); heavy solid line, fit to current data; dash-dot-dot line, Hippler et al.⁶ (~0.5 bar); dashed line, Braun-Unkshoff et al.⁷ (~2 bar) and Baulch et al.;²³ dotted line, Jones et al.¹⁰ (~10–12 bar); dash-dot line, Rao and Skinner⁸ (~0.6 bar). The two lines that are in agreement with the results of this study and are somewhat obscured by overlap in the figure are those of Hippler et al.⁶ and Braun-Unkshoff et al.⁷

imately an order of magnitude and therefore probably have uncertainties of at least an order of magnitude if not greater, and the rate coefficient determinations of Rao and Skinner⁸ are probably in error because of difficulties in determination of the initial reactant concentrations in their low-concentration H-atom ARAS measurements. The current rate coefficient determinations have significantly less uncertainty because of the low concentrations used and high sensitivity of the laser absorption technique.

On the basis of studies of falloff in toluene decomposition,^{12,24} we estimate that k_1 is within 30% of the high-pressure limit at the highest temperatures (~1730 K) of this study and is in the high-pressure limit at the lowest temperatures (~1430 K). Unfortunately, because the C_7H_6 decomposition product is of unknown structure (i.e., the transition state is of unknown structure), an RRKM/master equation calculation cannot be performed to extrapolate the rate coefficient experimental determinations to the high-pressure limit.

Conclusions

The decomposition of benzyl radicals has been studied under highly dilute concentrations at temperatures ranging from 1430 to 1730 K and at total pressures of 1.5 bar using shock wave heating and ultraviolet absorption of benzyl at 266 nm. Benzyl iodide was used as a benzyl precursor, providing instantaneous yields of benzyl following reflected shock heating. The 266 nm absorption traces allowed determination of the decomposition rate coefficient from the quasi-first-order decay in the absorbance and determination of the benzyl absorption cross-section at 266 nm by extrapolation of the steady decay in the absorbance to $t = 0$. The low concentrations used (50 and 100 ppm benzyl iodide/Ar) and the high levels of signal-to-noise provided by the laser absorption technique allowed for the determination of k_1 with an uncertainty of $\pm 25\%$ and determination of the 266 nm absorption cross-section with an uncertainty of $\pm 10\%$. The rate coefficient determinations are in excellent agreement with the previous rate determinations made by Hippler et al.⁶ and Braun-Unkshoff et al.⁷ Additionally, the development of a quantitative laser absorption diagnostic for benzyl will allow for future investigations of reactions involving benzyl radicals important in aromatic oxidation and pyrolysis systems.

Acknowledgment. This work was supported by the Chemical Sciences Division, Office of Basic Energy Sciences, U. S. Department of Energy.

References and Notes

- Smith, R. D. *J. Phys. Chem.* **1979**, *83*, 1553.
- Astholz, D. C.; Durant, J.; Troe, J. *Proc. Combust. Inst.* **1981**, *18*, 885.
- Astholz, D. C.; Troe, J. *J. Chem. Soc., Faraday Trans. 2* **1982**, *78*, 1413.
- Müller-Markgraf, W.; Troe, J. *Proc. Combust. Inst.* **1986**, *21*, 815.
- Müller-Markgraf, W.; Troe, J. *J. Phys. Chem.* **1988**, *92*, 4899.
- Hippler, H.; Reihs, C.; Troe, J. *Z. Phys. Chem. (Neue Folge)* **1990**, *167*, 1.
- Braun-Unkshoff, M.; Frank, P.; Just, Th. *Ber. Bunsen-Ges. Phys. Chem.* **1990**, *94*, 1417.
- Rao, V. S.; Skinner, G. B. *Proc. Combust. Inst.* **1986**, *21*, 809.
- Colket, M. B.; Seery, D. J. *Proc. Combust. Inst.* **1994**, *25*, 883.
- Jones, J.; Bacskay, G. B.; Mackie, J. C. *J. Phys. Chem. A* **1997**, *101*, 7105.
- Fröchtenicht, R.; Hippler, H.; Troe, J.; Toennies, J. P. *J. Photochem. Photobiol., A* **1994**, *80*, 33.
- Eng, R. A.; Gebert, A.; Goos, E.; Hippler, H.; Kachiani, C. *Phys. Chem. Chem. Phys.* **2002**, *4*, 3989.
- Ikeda, N.; Nakashima, N.; Yoshihara, K. *J. Phys. Chem.* **1984**, *88*, 5803.
- Hippler, H.; Troe, J. *J. Phys. Chem.* **1990**, *94*, 3803.
- Brouwer, L. D.; Müller-Markgraf, W.; Troe, J. *J. Phys. Chem.* **1988**, *92*, 4905.
- Baulch, D. L.; Cobos, C. J.; Cox, R. A.; Frank, P.; Hayman, G.; Just, Th.; Kerr, J. A.; Murrells, T.; Pilling, M. J.; Troe, J.; Walker, R. W.; Warnatz, J. *J. Phys. Chem. Ref. Data* **1994**, *23*, 847.
- Baulch, D. L.; Cobos, C. J.; Cox, R. A.; Esser, C.; Frank, P.; Just, Th.; Kerr, J. A.; Pilling, M. J.; Troe, J.; Walker, R. W.; Warnatz, J. *J. Phys. Chem. Ref. Data* **1992**, *21*, 411.
- Litzinger, T. A.; Brezinsky, K.; Glassman, I. *Combust. Flame* **1986**, *63*, 251.
- Heckmann, E.; Hippler, H.; Troe, J. *Proc. Combust. Inst.* **1996**, *26*, 543.
- Hippler, H.; Reihs, C.; Troe, J. *Proc. Combust. Inst.* **1990**, *23*, 37.
- Kee, R. J.; Rupley, F. M.; Miller, J. A. *Chemkin-II: A Fortran Chemical Kinetics Package for the Analysis of Gas-Phase Chemical Kinetics*; Sandia Report No. SAND89-8009.UC-4001; Sandia National Laboratory, Livermore, CA, 1989.
- Lutz, A. E.; Kee, R. J.; Miller, J. A. *Senkin: A Fortran Program for Predicting Homogeneous Gas-Phase Chemical Kinetics with Sensitivity Analysis*; Sandia Report No. SAND87-8248.UC-4; Sandia National Laboratory, Livermore, CA, 1988.
- Baulch, D. L.; Bowman, C. T.; Cobos, C. J.; Cox, R. A.; Just, Th.; Kerr, J. A.; Pilling, M. J.; Stocker, D.; Troe, J.; Tsang, W.; Walker, R. W.; Warnatz, J. *J. Phys. Chem. Ref. Data* In press.
- Oehlschlaeger, M. A.; Davidson, D. F.; Hanson, R. K. To be published.